Available online at www.sciencedirect.com
ScienceDirect
Carbohydrate Polymers 72 (2008) 261–271
Carbohydrate Polymers
www.elsevier.com/locate/carbpol

Modified chitosan and calcium alginate biopolymer sorbents for removal of nickel (II) through adsorption

Y. Vijaya [a], Srinivasa R. Popuri [b], Veera M. Boddu [c], A. Krishnaiah [a,*]

[a] *Biopolymers and Thermophysical Laboratories, Department of Chemistry, Sri Venkateswara University, Tirupati 517 502, India*
[b] *Department of Chemistry, National Chung-Hsing University, Taichung 40227, Taiwan, ROC*
[c] *U.S. Army Construction Engineering Research Laboratory, Engineer Research and Development Centre, Champaign, IL 61826, USA*

Received 16 April 2007; received in revised form 4 August 2007; accepted 10 August 2007
Available online 17 August 2007

Abstract

Removal of nickel (II) from aqueous solutions through adsorption on to biopolymer sorbents, such as calcium alginate (CA), chitosan coated calcium alginate (CCCA) and chitosan coated silica (CCS), was studied using equilibrium batch and column flow techniques. The biosorbents were characterized by FTIR, SEM, TGA and surface area analysis. The extent of adsorption was found to be a function of the pH of the solution, contact time, sorbate concentration and adsorbent dose. The optimum pH was found to be 5.0. The adsorption of Ni (II) ions on CA was comparatively higher than CCCA and CCS. Adsorption of Ni (II) on to the biopolymers followed pseudo-second order kinetics. The equilibrium adsorption data for Ni (II) on CA, CCCA and CCS were fitted to Freundlich, and Langmuir Isotherms. The maximum monolayer adsorption capacity of the biosorbents (CA, CCCA and CCS), as obtained from Langmuir adsorption isotherm, was found to be 310.4, 222.2 and 254.3 mg/g, respectively. Breakthrough curves were obtained for adsorption of Ni (II) on all the three adsorbents through column flow technique. The Ni (II) loaded biosorbents were regenerated using 0.1 M EDTA solution.

Keywords: Biosorption; Nickel; Chitosan; Calcium alginate; Silica

1. Introduction

The presence of heavy metal ions from the transition series, viz, Cu, Fe, Ni, and Pb etc. in the environment was of major concern due to their toxicity to many life forms. Many industrial processes such as mining, electroplating, dyeing, paper and petroleum produce wastewater streams containing heavy metals which are toxic to living organisms (Gupta, Gupta, & Sharma, 2001). Unlike organic pollutants, metallic pollutants released into the environment tend to persist indefinitely, circulating and eventually accumulating throughout the food chain thus posing a serious threat to animals and man. Since the metal ions must be removed before discharge, an economical process for removing low levels of these heavy metals from such a large volume of waste stream was important. Precipitation, oxidation and reduction, ion exchange, filtration, reverse osmosis, electro-chemical removal, and evaporative recovery can all potentially be used to treat industrial effluents for metals (Chong & Volesky, 1995; Leusch, Holan, & Volesky, 1995; Volesky, 1999). These methods are inefficient for heavy metal contaminants at tracer levels. Wastewater discharge from electroplating, electronics and metal cleaning industries often contain high concentrations of Ni (II) ions and causes serious water pollution.

Many biopolymers such as sodium alginate, chitosan extracted from microalgae (Da Costa & Leite, 1991), shrimp, crab, some fungi (Bosinco, Dambies, Guibal, Roussy, & Le Cloirec, 1997; Jang, Lopez, Eastmen, & Pryfogle, 1991) are known to bind metal ions strongly and could be used for heavy metal adsorption. Biopolymers are non-toxic, selective, efficient and inexpensive and thus highly competitive with ion-exchange resins and activated carbon. Immobilizing biomass in a biopolymeric matrix may also improve biomass performance, biosorption

* Corresponding author.
E-mail address: abburikrishnaiah@gmail.com (A. Krishnaiah).

0144-8617/$ - see front matter © 2007 Elsevier Ltd. All rights reserved.
doi:10.1016/j.carbpol.2007.08.010

capacity and facilitate the separation of biomass from metal-bearing solutions. Alginate is a linear copolymer of a-L-guluronate (G) and a-D-mannuronate (M), which constitutes 10–40% of the dry weight of all species of brown algae (Volesky, 2003). The gelation properties of alginate can be attributed to the simultaneous binding of the divalent cations such as Ca^{2+} to different chains of a-L-guluronate blocks. As a result of their configuration, these chains form electronegative cavities capable of holding the cations via ionic interactions, resulting in cross-linking of the chains into a structure resembling an "egg box" (Grant, Morris, Rees, Smith, & Thom, 1973). Due to its ability to form stable structures, cross-linked alginate has been used for the removal of heavy metal from wastewater (Holan, Volesky, & Prasetyo, 1993; Kuyucak & Volesky, 1989; Romero-Gonzalez, Williams, & Gardiner, 2001). Although it has been demonstrated that the alginates present in algae are capable of binding heavy metals through carboxyl groups (Chen & Yiacoumi, 1997; Ibãnez & Umetsu, 2002; Konishi, Asai, Midoh, & Oku, 1993; Mimura, Ohta, Akiba, & Onodera, 2001), very few studies have been conducted on the potential use of alginates as a sorbent for heavy metal removal from aqueous solutions.

Chitosan appears to be a more economically attractive sorbent for removal of metallic ions from water, since it is obtained from chitin the second most abundant polymer in nature next to cellulose. Furthermore, chitosan has many useful features such as biocompatibility, biodegradability, and anti-bacterial properties. Chitosan is effective in the uptake of transition metals since the amino groups on chitosan chains serve as coordination sites (Muzzarelli, 1983). Several methods have been used to modify raw chitosan flakes either by physical (Veera, Krishnaiah, Jonathan, & Edgar, 2003; Yang & Yuan, 2001; Zhang & Chen, 2002) or chemical (Ho, Ng, & Me Kay, 2001; Hsalah, Weber, & Vera, 2000; Zouboulis, Matris, Lanara, & Nescovic, 1997) modifications in order to improve pore size, mechanical strength, chemical stability, and biocompatibility.

In the present study, new biosorbents were developed by coating chitosan, a glucosamine biopolymer, on calcium alginate and silica to overcome some of the problems associated with the use of pure chitosan. The aim of the work was to prepare calcium alginate (CA), chitosan coated calcium alginate (CCCA) and chitosan coated silica (CCS) and to determine the ability of these biosorbents in removing nickel (II) ion from aqueous medium under batch equilibrium and column flow experimental conditions. Further the biosorbents were characterized by FTIR, SEM, TGA and surface area analysis to understand the surface morphology.

2. Experimental

2.1. Materials

Analytical grade nickel ammonium sulphate was purchased from S.D. Fine Chemicals for nickel (II) ion source. Hydrochloric acid and sodium hydroxide used for pH adjustment and for the preparation of beads were obtained from Aldrich Chemical Company and Chemical Drug House Ltd. Sodium alginate was obtained from Loba Chemie, and acetic acid and calcium chloride were purchased from S.D. Fine Chemicals. Chitosan, with an average molecular weight of 500,000 and 84% of degree of deacetylation, and silica gel were obtained from Aldrich Chemical Company. Double distilled water of conductivity <0.02 S/cm was used throughout this work.

2.2. Preparation of biosorbent beads

2.2.1. Calcium alginate beads

Sodium alginate solution was prepared by dissolving and gently heating 4 g of alginate in 96 ml of water. The solution was then dropped into 2% calcium chloride solution through the tip of the transfer pipette. The drops of sodium alginate solution gelled into 3.5 ± 0.1 mm diameter beads upon contact with calcium chloride solution. The beads were kept in contact with calcium chloride solution for 4 h, which lead to the formation of insoluble and stable beads. Water soluble sodium alginate was converted to water insoluble calcium alginate (CA) beads using $CaCl_2$ solution. The beads were rinsed with double distilled water and dried until the water was completely evaporated. It was observed that the size of the beads decreases on drying. Five different beads of the completely dried sample were taken randomly and the size of the each bead was measured by using the micrometer screw gauge with an accuracy of ± 0.01 mm. The average size of the bead was found to be 2.05 mm.

2.2.2. Chitosan coated calcium alginate

The calcium alginate beads were dropped in to a 4% chitosan gel, prepared by dissolving 4 g of chitosan in 100 ml of 2% acetic acid solution and stirred for about 12 h. Then the beads covered with chitosan were transferred into a 500 ml of 0.1 M NaOH solution and allowed to stand for about 4 h. Generally, chitosan is soluble in weak acids and insoluble in alkaline medium. The beads were removed from the alkali, thoroughly washed with double distilled water until the washings were neutral and dried.

2.2.3. Chitosan coated silica

Ten grams of silica, washed with 2% acetic acid solution, were added to 100 ml of 4% chitosan gel while stirring with a magnetic stirrer for 4 h. This process led to the formation of a silica/chitosan suspension. This suspension was dropped into 500 ml of 0.1 M NaOH solution while stirring to neutralize excess acid. The suspension was converted into pellets. The pellets were washed with double distilled water until the washings were neutral. The material was crushed, sieved and particles with 100 mesh size were used as the biosorbent.

2.3. Equilibrium adsorption studies

An adsorbate stock solution of 1000 mg/L of nickel (II) was prepared by dissolving 6.73 g of nickel ammonium sulphate in double distilled water. This stock solution was diluted to the required concentration (50–500 mg/L of Ni (II)). Equilibrium batch adsorption experimental studies were carried out with known weight (150 mg) of adsorbent and 100 ml of nickel (II) stock solution of desired concentration at optimum pH (5.0) in 125 ml stopper bottles. The bottles were agitated at 160 rpm for 150 min time intervals at room temperature in a mechanical shaker. After attaining equilibrium, the biosorbent was separated by filtration and the aqueous-phase concentration of metal was analyzed with Atomic Absorption Spectrophotometer (Perkin-Elmer 2380).

The equilibrium uptake capacity for each sample was calculated according to mass balance on nickel ions;

$$q_e = \left(\frac{C_i - C_e}{m}\right) V \quad (1)$$

where C_i and C_e were, respectively, initial and equilibrium concentrations of metal ion, m was the mass of adsorbent and V was volume of the solution in liters. Experiments were conducted with metal ion solution in the absence of adsorbent and it was found that there was no metal adsorption by the walls of the container.

2.4. Column adsorption studies

Column flow adsorption experiments were conducted in a glass column of about 2.5 cm internal diameter and 10 cm length. The column was filled with a known weight of the adsorbent while tapping the column such that the column was filled without voids. The adsorbate solution was allowed to flow through the column at a constant flow rate (2 ml/min) throughout the experiment. The pH of the inlet solution was adjusted to 5.0 at the start of the experiment. The effluent solution was collected at different time intervals and the concentration of Ni (II) ion in the effluent solution was monitored by Atomic Absorption Spectrophotometer. The solutions were diluted appropriately prior to analysis. Samples at 10 min time intervals from the start of the experiment were collected for analysis. Column studies were conducted for the three adsorbents (CA, CCCA and CCS). Breakthrough curves for each adsorbent individually were obtained by plotting the volume of the solution against the ratio of the concentration of effluent at any time (C_e) to that of the inlet solution (C_0), C_e/C_0.

2.5. Desorption studies

The desorption (recovery) studies are very important since the economic success of the adsorption process depends on the regeneration of adsorbent. There are several methods for desorption of the adsorbate from the loaded adsorbents. In the present study, the elution method with solvent was used to remove the adsorbed metal ions from adsorbents. Several solvents/solutions were tried to regenerate the biosorbents. Out of several solvents/solutions, 0.1 M ethylenediamine tetraacetic acid (EDTA) solution was found to be effective in desorbing Ni (II) ions from the loaded adsorbents. The column was regenerated using 0.1 M EDTA solution, when the concentration of the effluent solution was close to the inlet concentration. The remaining aqueous solution was drained from the column by pumping air. Then EDTA solution was passed in to the column at a fixed flow rate and the concentration of the solution coming out of the column was monitored.

2.6. Characterization of biosorbents

The biosorbents were characterized using FTIR spectra, SEM micrograph, thermogravimetric and surface analysis. FTIR spectra of biopolymers were recorded in a Perkin-Elmer-283B FTIR spectrometer over the wave range 4000–400 cm^{-1}. The samples were prepared as KBr discs. SEM photographs were taken with JSM 6700F Scanning Microscope to examine the morphology and surface structure of the beads at the required magnification at room temperature. The beads were deposited on a brass hold and sputtered with a thin coat of gold under vacuum. Acceleration voltage used was 20 kV with the secondary electron image as a detector. Thermal gravimetric analyses (TGA) were performed on freeze-dried CA, CCCA and CCS samples using Mettler Thermal Analyzer TG-50 in the temperature range of 30–400 °C at a heating rate of 10 C/min with nitrogen flushed at 200 ml/min. Surface area of the biosorbents was measured by single point BET (Brunauer, Emmett and Teller) method using thermal conductivity detector (Carlo Erba Soptomatic – 1800) within the range of 0.1–2000 $m^2\ g^{-1}$ and with the sample size of 2–10 mg. Pycnomatic ATC was uniquely designed for density measurement of solid and powder samples. Pore volume of the biosorbent samples was measured using Pycnomatic ATC (Thermo Electronic Corporation).

3. Result and discussion

3.1. FTIR spectra

The FTIR spectra of CA, CCCA and CCS are shown in Fig. 1 in both pristine and metal loaded forms. The IR spectrum of pristine calcium alginate (Fig. 1a) shows absorption bands at 3430 cm^{-1} (OH stretching), 1618 cm^{-1} (COO^- asymmetric stretching), and 1429 cm^{-1} (COO^- symmetric stretching). The bands at 1125 cm^{-1} are due to the –C–O stretching of ether groups and the bands at 1065 cm^{-1} are assigned to the –C–O stretching of alcoholic groups. Fig. 1b shows the FTIR spectrum of CA loaded with Ni (II) ions. An interesting phenomenon is the sharp shift in the position and intensity of the bands after metal binding. The FTIR spectrum of CCCA biosorbent in Fig. 1c indicates the presence of predominant peaks

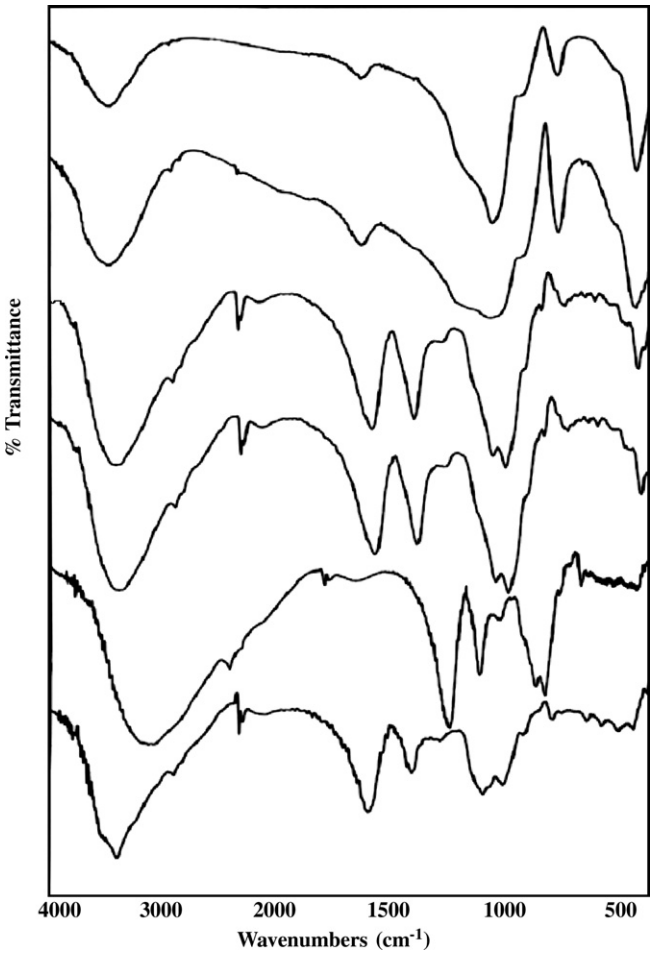

Fig. 1. FTIR spectra of (a) CA, (b) CA loaded with Ni (II), (c) CCCA, (d) CCCA loaded with Ni (II), (e) CCS, (f) CCS loaded with Ni (II).

at 3352 cm^{-1} (–OH and –NH stretching vibrations), 2987 cm^{-1} (–CH stretching vibration), 1568 cm^{-1} (–NH bending vibration), 1393 cm^{-1} (–NH deformation vibration), and 1065 cm^{-1} (–CO stretching vibration). This reveals that all functional groups originally present on chitosan and alginate are still present even after coating process and are available for interaction with Ni (II) ions. Fig. 1d represents the FTIR spectra of Ni (II) loaded CCCA, indicating the shift in the position and intensity of the peaks upon metal binding. Chitosan coated silica shows a peak (Fig. 1e) at the wave number 797 cm^{-1} (C–H group out of plane). A broad peak at around 1092 cm^{-1} may be due to the merging of peaks relating to Si–O–Si, Si–O–H, C–O groups. Another broad peak around 3439 cm^{-1} is attributed to –NH and O–H stretching vibrations. The FTIR spectrum of Ni (II) loaded CCS (Fig. 1f) indicates the considerable change in the position and intensity of the peaks. From these observations it may be concluded that $–NH_2$, –OH, –CO and –SiO act as binding sites for Ni (II) ion adsorption on the biosorbents. The study of Chui et al. (Chui, Mok, Ng, Luong, & Ma, 1996) confirmed that the amino groups of chitosan are the major effective binding sites for metal ions, forming stable complexes by coordination. The nitrogen electrons present in the amino groups can establish dative bonds with transitional metal ions. Some hydroxyl groups in these biopolymers may function as donors. Hence, deprotonated hydroxyl groups are involved in the coordination with metal ions (Lerivrey, Dubois, Decock, Micera, & Kozlowski, 1986). It was established that chitosan forms chelates with metal ions by releasing hydrogen ions (Inoue, Baba, Yoshizuka, Noguchi, & Yoshizaki, 1988). Formation of a complex between chitosan and Ni (II) is shown in Fig. 2.

3.2. Surface morphology

The SEM images of the surface of CA, CCCA and CCS, shown in Fig. 3, display a rough structure on surface with a large surface area. An examination of the SEM micrographs (Fig. 3a and b) indicates the presence of many pores and also some cracks on the surface of the biosorbents. It also shows the surface condition on chitosan coated beads is somewhat swollen during the contact with nickel ion solution. The results from TGA are presented in Figs. 4–6 for CA, CCCA and CCS in the form of thermograms. Chitosan has two main decomposition stages with one starting at 238 °C and another starting at around 320 °C (Ding, Qing Lian, Samuels, & Polka, 2003). Thermal behavior of CA and CCCA is not much different, where as CCS behaves differently. The two weight losses in the case of CA and CCCA occur at around 235 °C (about

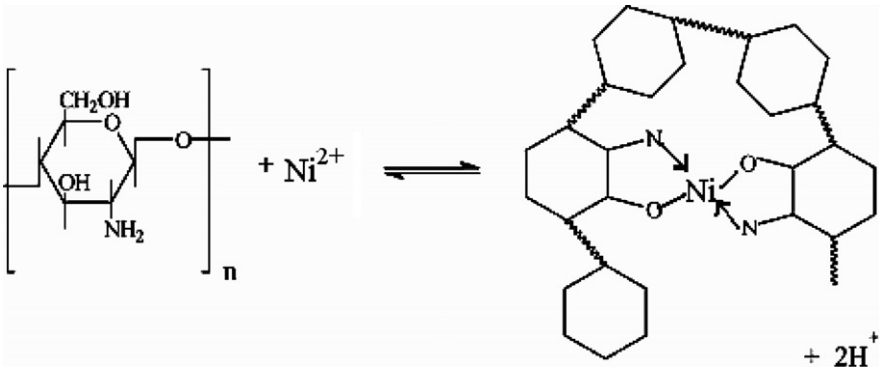

Fig. 2. Formation of complexation between chitosan and Ni (II).

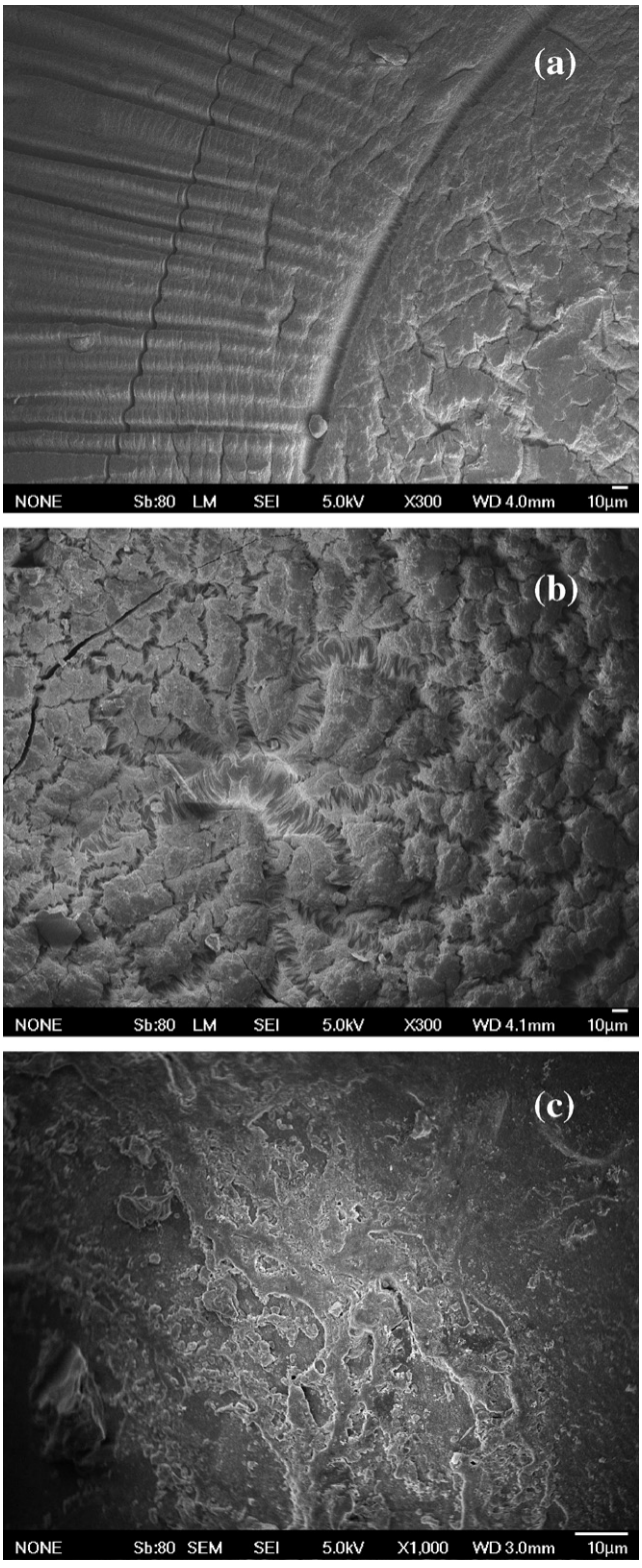

Fig. 3. SEM images of (a) CA, (b) CCCA and (c) CCS.

16%) and 318 °C (about 40%). The thermogram of CCS shows a broad transition with a relatively less weight loss. The weight loss is about 3% around 150 °C and about 6% at 360 °C. Thermogram of CCS indicates that about 8% of chitosan is coated on silica. From the TGA analyses of the biosorbents, it may be concluded that the biosorbents could be used even at higher temperatures in water treatment.

Surface area and pore volume values were presented in Table 1. Among the three biosorbents, the CA possesses high surface area and pore volume when compared to the other two sorbents. Obviously the metal uptake capacity of this sorbent will be high due to its free hydroxyl groups.

3.3. Effect of pH

The most important parameter influencing the biosorption rate and capacity is the pH of the biosorption medium. To evaluate the effect of pH on nickel (II) sorption capacity on the biopolymer adsorbents, experiments were conducted with 100 ml of 100 mg/L of metal solution containing 150 mg of adsorbent in the pH range 2–6 at room temperature. It was observed that biosorption rate increases as the pH of adsorption medium increases. The influence of pH was not studied beyond 6.0 due to the formation of precipitate. Fig. 7 depicts the effect of pH on the adsorption of Ni (II) ion on CA, CCCA and CCS. The optimum pH for all the three sorbents was found to be 5.0 for nickel (II) ion adsorption.

The effect of pH on adsorption capacity may be discussed on the basis of the nature of the chemical interactions of Ni (II) ions with the biosorbents. The carboxylic (–COOH) and amino ($–NH_2$) groups present on the biosorbents are responsible for the binding of nickel (II). At lower pH, the carboxylic groups retain their protons and amino groups get protonated, thereby, reducing the probability of binding to any positively charged ions. Whereas at higher pH (above 4.0), the COO^- ions, formed due to dissociation of carboxylate groups, and the free amino groups attract the positively charged Ni (II) ions. This results in an increase of adsorption. According to Low et al. (Low, Lee, & Tan, 1995), at low pH values the surface of adsorbent would be closely associated with hydronium ions (H_3O^+), which hinder the access of the metal ions to the surface functional groups. Consequently, the percentage of metal ion removal is relatively small at lower pH. The low level of nickel (II) uptake at lower pH values could also be attributed to the increased concentration of hydronium (H_3O^+) ions competing for nickel (II) binding sites on the biomass.

3.4. Adsorption kinetics

To understand the effect of time on the extent of adsorption, equilibrium concentrations of Ni (II) ions were determined at different time intervals with initial concentrations of 100, 250 and 500 mg/L, keeping the pH and amount of biosorbent constant. The results are graphically presented in Figs. 8–10 for CA, CCCA and CCS. The adsorption efficiency of all the three biosorbents (CA, CCCA and CCS) increased with time and attained equilibrium within 90 min. The data were used to study the kinetics of adsorp-

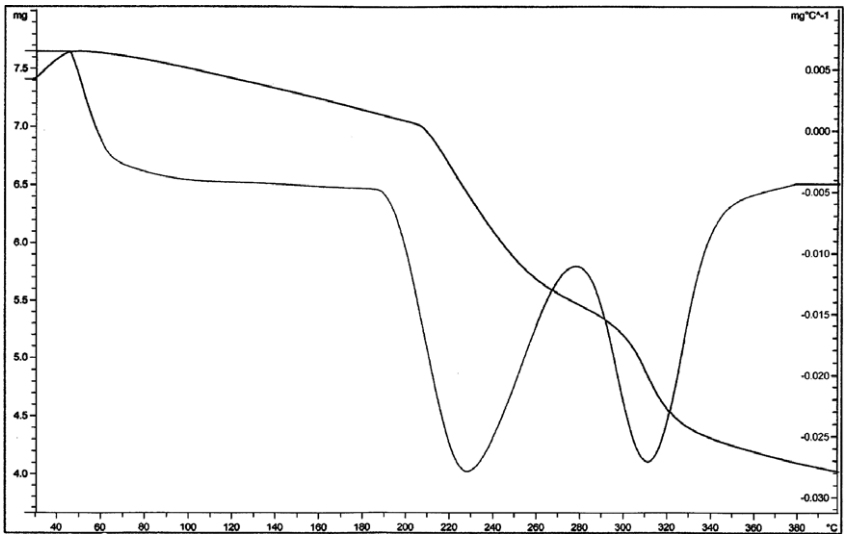

Fig. 4. Thermogravimetric curve of calcium alginate.

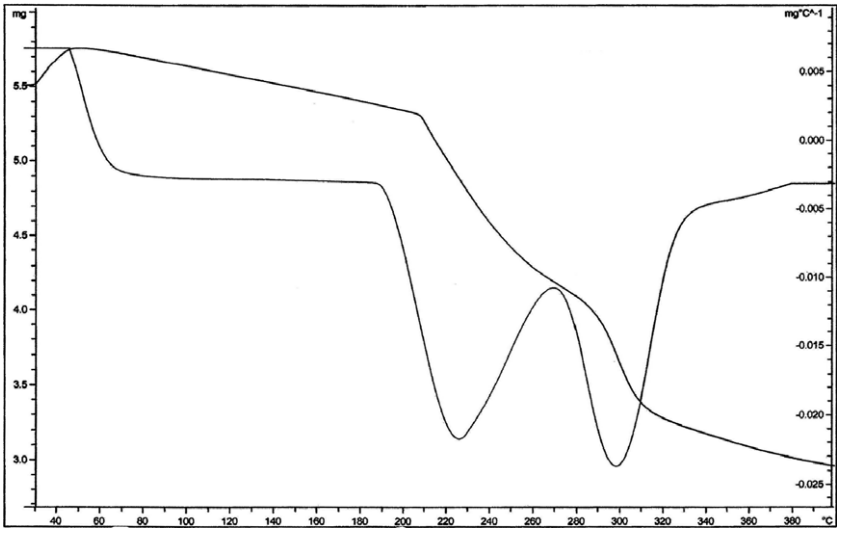

Fig. 5. Thermogravimetric curve of chitosan coated calcium alginate.

tion of Ni (II) on biosorbents. Kinetics of adsorption using different models was studied by many workers (Aksu, 2002; Donmez & Aksu, 2002; Rangsayatorn, Upatham, Kruatrachue, Pokethitiyook, & Lanza, 2002). In order to investigate the mechanism of sorption, the rate constants for the nickel ion adsorption were determined by using Lagergren and a pseudo-second order equations.

The Lagergren first order kinetic equation is

$$\frac{dq_e}{dt} = k_1(q_e - q_t) \tag{2}$$

Linearized form of the above equation is

$$\log(q_e - q_t) = \log q_e - \left(\frac{k_1}{2.303}\right)t \tag{3}$$

where q_e and q_t are the amounts of solute adsorbed per unit mass of the adsorbent (mg/g) at equilibrium time and time t (min), respectively, and k_1 is the rate constant (min^{-1}). The straight line plots of $\log(q_e - q_t)$ against t are used to determine the rate constant, k_1 and correlation coefficients, R^2 for different concentrations.

The pseudo-second order equation (Ho, 2003) may be expressed as

$$\frac{dq_e}{dt} = k_2(q_e - q_t)^2 \tag{4}$$

Linearized form of the above equation is

$$\frac{t}{q_t} = \frac{1}{k_2 q_e^2} + \frac{t}{q_e} \tag{5}$$

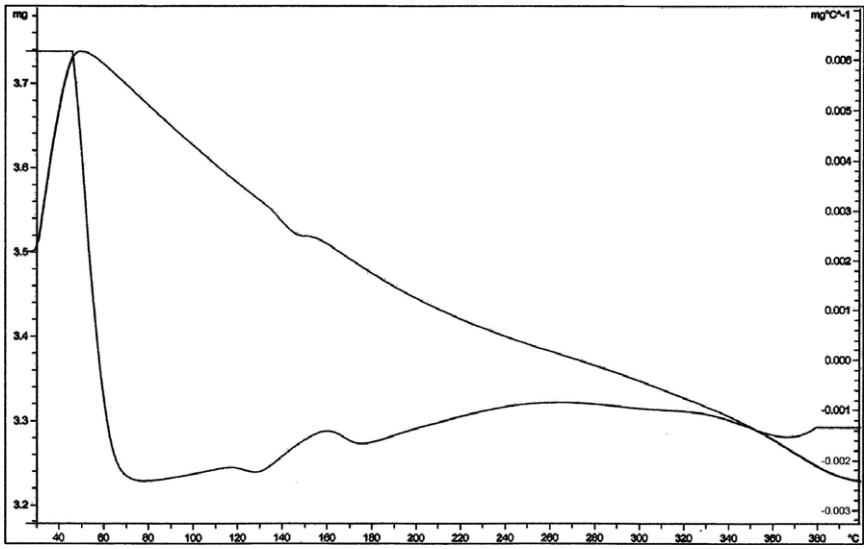

Fig. 6. Thermogravimetric curve of chitosan coated silica.

Table 1
Surface area and pore volume values of the adsorbents

Biosorbent	Pore volume (cc)	Surface area (m^2/g)
CA	0.231	178.3
CCCA	0.202	144.6
CCS	0.224	160.8

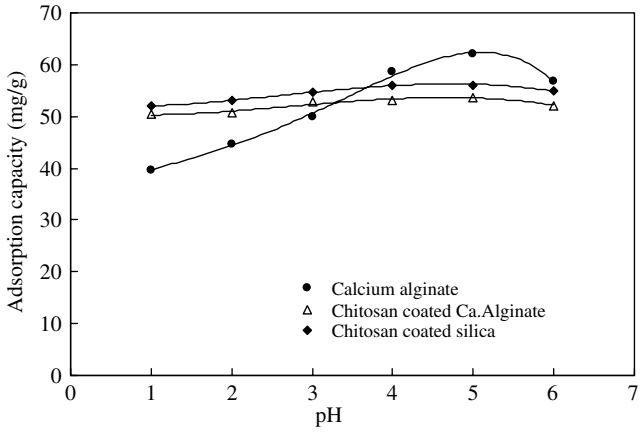

Fig. 7. Effect of pH on biosorption of Ni (II) on biopolymer sorbents.

where k_2 is the rate constant of second order adsorption ($g\,mg^{-1}\,min^{-1}$). The straight line plots of t/q_t against t are used to obtain rate parameters.

The rate constants of Lagergren and pseudo-second order kinetic models are shown in Tables 2 and 3. The first order kinetic process has been used for the description of reversible equilibrium between liquid and solid phases whereas, the second order kinetic model assumes that the rate limiting step may be chemical adsorption (Ho & McKay, 2000). In many cases, the adsorption data are well correlated by the second order equation (Wu, Tseng, & Juang, 2000). An examination of the values in the tables

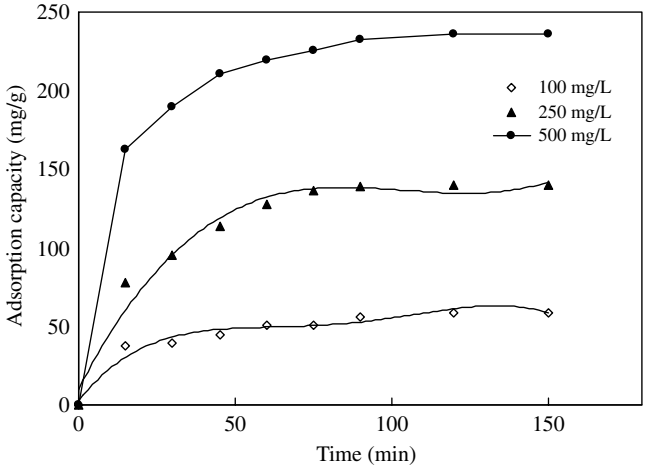

Fig. 8. Effect of time on biosorption of Ni (II) on calcium alginate.

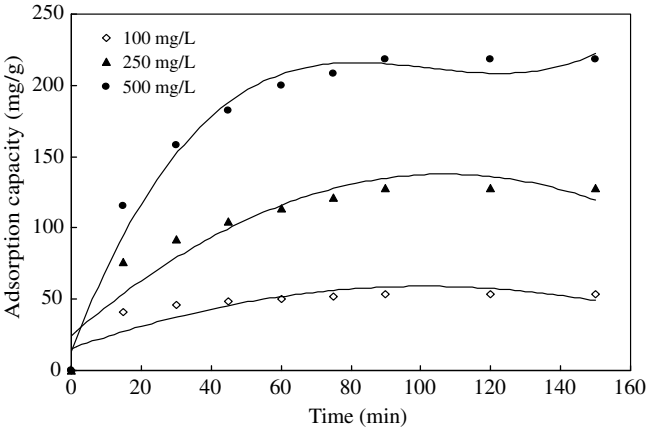

Fig. 9. Effect of time on biosorption of Ni (II) on chitosan coated calcium alginate.

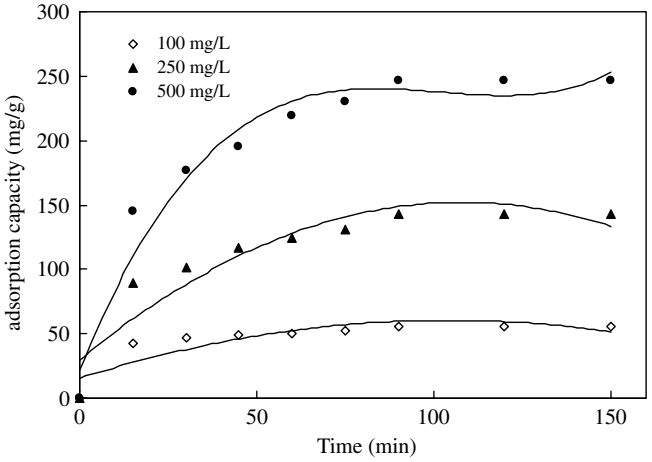

Fig. 10. Effect of time on biosorption of Ni (II) on chitosan coated silica.

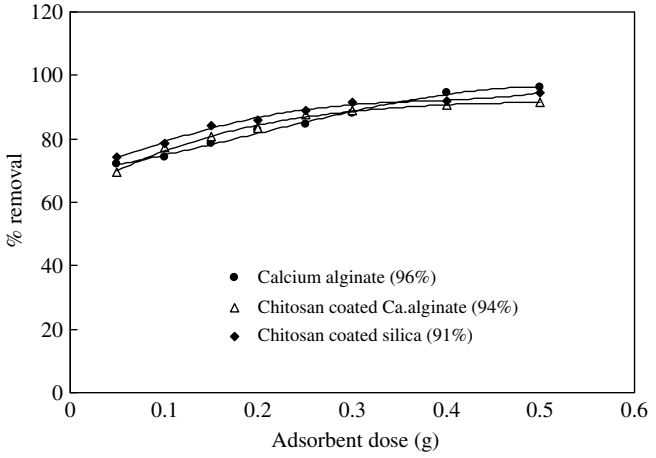

Fig. 11. Effect of adsorbent dose on percent removal of Ni (II) ion using CA, CCCA and CCS.

Table 2
Lagergren first order rate constants for adsorption of Ni (II) on CA, CCCA and CCS

Biosorbent	Concentration of nickel (II) solution (mg/L)					
	100		250		500	
	k_1 (min^{-1})	R^2	k_1 (min^{-1})	R^2	k_1 (min^{-1})	R^2
CA	0.024	0.986	0.040	0.988	0.052	0.982
CCCA	0.033	0.987	0.034	0.983	0.038	0.997
CCS	0.020	0.991	0.025	0.994	0.030	0.985

Table 3
Pseudo second order rate constants for adsorption of nickel (II) on CA, CCCA and CCS

Biosorbent	Concentration of nickel (II) solution (mg/L)					
	100		250		500	
	k_2 (mg^{-1} g min^{-1})	R^2	k_2 (mg^{-1} g min^{-1})	R^2	k_2 (mg^{-1} g min^{-1})	R^2
CA	1.15×10^{-3}	0.988	2.81×10^{-3}	0.995	1.96×10^{-3}	0.996
CCCA	0.40×10^{-3}	0.999	0.48×10^{-3}	0.997	0.44×10^{-3}	0.997
CCS	0.20×10^{-3}	0.997	0.27×10^{-3}	0.996	0.23×10^{-3}	0.996

indicates that the adsorption of Ni (II) on the biosorbents follows the second order kinetic model. In many cases the first order equation of Lagergren is generally applicable over the initial stage of adsorption process and fails to represent the adsorption data over the whole range of contact time.

3.5. Effect of biosorbent dose

The dependence of Ni (II) sorption on biosorbent dose was studied by varying the amount of adsorbent from 0.05 to 0.5 g while keeping all other variables (pH, agitation time and concentration (100 mg/L)) constant. The results are presented in Fig. 11, which indicates that removal efficiency of the adsorbent increases with increasing adsorbent dose. This is expected due to the fact that the higher dose of adsorbent in the solution results in greater availability of exchangeable sites for the ions. The maximum nickel (II) ion removal efficiencies are 96% with CA, 94% with CCCA and 91% with CCS. This suggests that the Ni (II) ion can be removed effectively by using <1 gm of the biosorbent.

3.6. Adsorption isotherms

Out of several isotherm equations, the Freundlich and Langmuir isotherms were used to fit the experimental data. The variation of the extent of adsorption with concentration of Ni (II), included in Fig. 12, shows that the sorbents exhibit high metal uptake capacity at higher initial concentration. The Langmuir isotherm assumes a surface with homogeneous binding sites, equivalent sorption energies, and no interaction between sorbed species. In mathematical form, it is written as

$$q_e = \frac{Q^0 b C_e}{(1 + bC_e)} \tag{6}$$

$$\frac{1}{q_e} = \frac{1}{Q^0 b C_e} + \frac{1}{Q_0} \tag{7}$$

where q_e is the specific metal uptake, Q^0 the maximum adsorption capacity in mg/g, C_e the equilibrium concentration in mg/L, and b relates to the affinity of the sorbate for the binding sites expressed in L/mg.

The Freundlich isotherm is an empirical equation based on an exponential distribution of sorption sites and energies. In mathematical form, it is represented as

$$q_e = K_f C_e^{1/n} \tag{8}$$

$$\log q_e = \log K_f + \frac{1}{n} \log C_e \tag{9}$$

where K_f and $\frac{1}{n}$ are related to the sorbent capacity and sorption intensity, respectively.

Though both Langmuir and Freundlich isotherms are capable of representing the data satisfactorily (Figs. 13

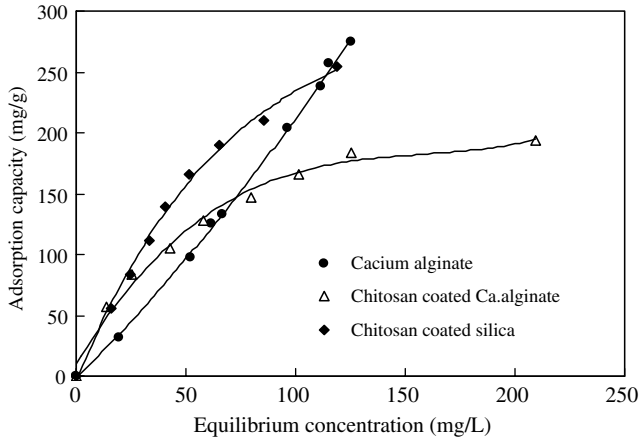

Fig. 12. Effect of initial metal ion concentration on adsorption of Ni (II).

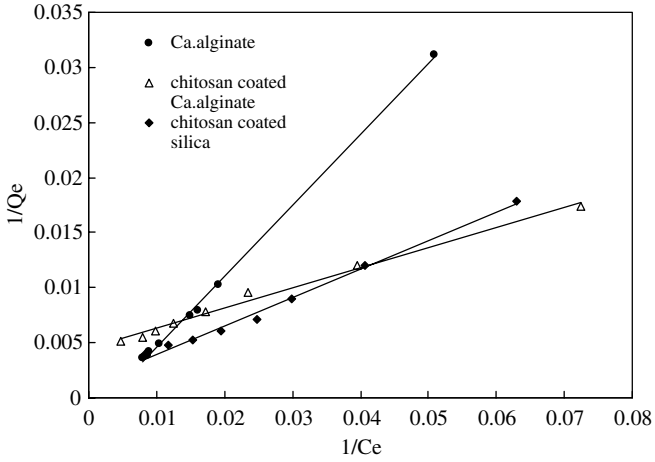

Fig. 13. Langmuir isotherm for Ni (II) biosorption on CA, CCCA and CCS.

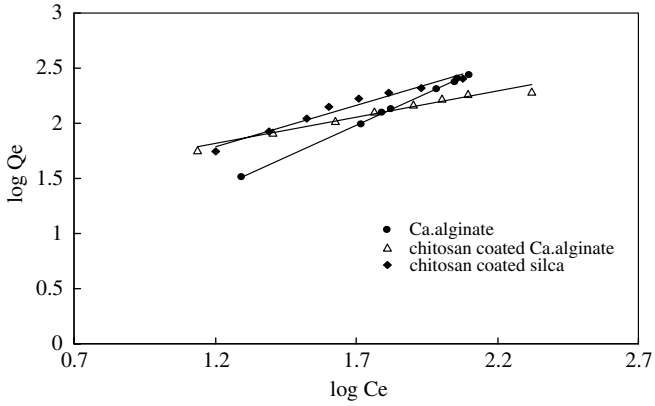

Fig. 14. Freundlich isotherm for Ni (II) biosorption on CA, CCCA and CCS.

and 14), the Langmuir model gives a better representation. The values of Langmuir and Freundlich constants are given in Table 4. The Langmuir parameter, b, can be used to predict the affinity between the sorbate and

Table 4
Langmuir and Freundlich isotherm constants for adsorption of nickel (II) on CA, CCCA and CCS

Biosorbent	Q^0 (mg/g)	b (L/mg)	R^2	K_F (L/g)	n	R^2
CA	310.4	0.36×10^{-2}	0.990	0.931	0.854	0.986
CCCA	222.2	0.24×10^{-1}	0.990	11.988	2.129	0.973
CCS	254.3	0.26×10^{-2}	0.994	7.693	1.325	0.976

sorbent using the dimensionless separation factor, R_L, defined by Hall et al. (Hall, Eagleton, Acrivos, & Vermeulen, 1966) as

$$R_L = \frac{1}{1 + bC_0} \tag{10}$$

where C_0 is the initial Ni (II) concentration (mg/L) and b is the Langmuir adsorption equilibrium constant (L/mg). If the R_L values are equal to zero or one, the adsorption is either linear or irreversible, and if the values are in between zero and one, adsorption is favorable to chemisorption. The values of R_L for sorption of nickel on CA, CCCA and CCS are less than 1 and greater than 0, indicating the favorable uptake of Ni (II) by all the biosorbents.

3.7. Column studies

Column adsorption studies were performed under the optimum conditions with a flow rate of 2 ml/min and inlet nickel (II) concentration of 100 mg/L. The total amount of nickel (II) adsorbed for a given feed concentration and flow rate was calculated from the area under the breakthrough curve. The maximum specific nickel (II) uptake is defined as the total amount of metal ion sorbed for a gram of biosorbent in the packed bed at the end of total flow time. Breakthrough curves were obtained by plotting the normalized concentration defined as the ratio of effluent nickel (II) ion concentration to inlet nickel (II) ion concentration (C_e/C_0) as a function of effluent volume.

Adsorption breakthrough curves obtained for different biosorbents are given in Fig. 15. As can be seen in

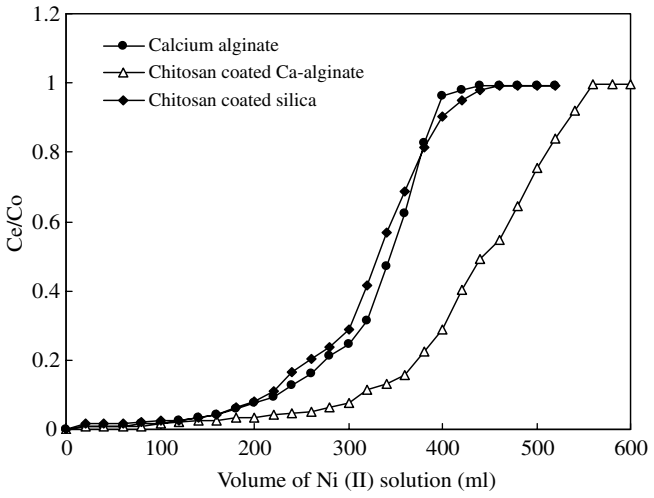

Fig. 15. Column break-through curves for adsorption of Ni (II) on CA, CCCA and CCS.

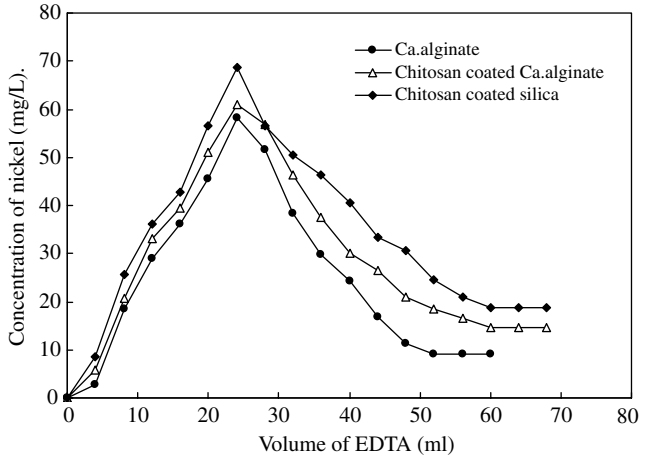

Fig. 16. Desorption curves of Ni (II) adsorbed on CA, CCCA and CCS.

Fig. 15, the outflow concentration profiles show that nickel removal was fast and highly effective during the initial phase. Subsequently, metal removal decreases, as a consequence of the progressive saturation of the binding sites. Such profiles depict a breakthrough curve similar to those observed by other authors (Aksu, Egretti, & Kutsal, 1999; Brady & Duncan, 1994; Huang, Haung, & Morehart, 1990). The concentration of Ni (II) ion in the effluent solution is almost zero up to about 220 ml. Afterwards it starts increasing and finally reaches the influent concentration. The adsorption capacity of the biomass in each column was obtained by dividing the concentration of metal adsorbed by the total amount of biomass used. The effective amount of Ni (II) retained by CA, CCCA and CCS are 39.6, 49.6 and 38.3 mg/g, respectively. It was reported in the literature that chitosan shows an adsorption capacity of 11.7 mg/g (Lima & Airoldi, 2004); blank alginate beads exhibit adsorption capacity of 25.6 mg/g (Abu Al-Rub, El-Naas, Benyahia, & Ashour, 2004); and iron imprinted silica and non-imprinted silica gel possess an adsorption capacity of 12.6 and 4.3 mg/g (Jiang, Chang, Zheng, He, & Hu, 2006), respectively. The adsorption capacity values reported in the present study are considerably higher than the above values reported in the literature. From this observation it may be concluded that the process of modification of the biopolymers resulted in an enhancement of adsorption capacity.

3.8. Desorption

When considering the choice of the eluent it is necessary to consider the efficiency of desorption as well as preservation of biosorption capacity of the biomass. Several solvents/solutions were tried in order to regenerate the column. Among them 0.1 M EDTA was proved to be a relatively effective eluent for desorption of nickel ions from the biosorbent with an optimum flow rate of 2 ml/min. The regeneration profiles of the biosorbents loaded with Ni (II) ions are shown in Fig. 16. EDTA is capable of removing about 43% of the metal ions adsorbed on the biomasses of CA, CCCA and CCS. Maximum desorption occurred in 30 min with 60 ml volume of 0.1 M EDTA.

4. Conclusions

In this study, calcium alginate (CA), chitosan coated calcium alginate (CCCA) and chitosan coated silica (CCS) were developed as biosorbents and characterized using FTIR spectra, SEM micrograph, thermograms and surface analysis. Adsorption of nickel (II) on CA, CCCA and CCS was investigated using batch equilibrium and column flow methods. The data demonstrated that the biomaterials are effective adsorbents for the removal of Ni (II) from aquatic medium. The adsorption of the metal ion depended on the amount of adsorbent, concentration of metal ions, agitation time, and pH of the metal solution. Maximum removal of nickel (II) on biopolymer sorbents was at pH 5.0. The equilibrium adsorption data were correlated well by Langmuir and Freundlich isotherm equations. The maximum monolayer adsorption capacity of CA, CCCA and CCS was 310.4, 222.2 and 254.3 for Ni (II), respectively. The actual Ni (II) uptake by the biosorbents developed in this study was much higher than that of chitosan, alginate and silica reported in the literature. Biosorption of Ni (II) ion followed the pseudo-second order kinetics.

References

Abu Al-Rub, F. A., El-Naas, M. H., Benyahia, F., & Ashour, I. (2004). Biosorption of nickel on blank alginate beads, free and immobilized algal cells. *Process Biochemistry, 39*, 1767–1773.

Aksu, Z. (2002). Determination of the equilibrium, kinetic and thermodynamic parameters of the batch biosorption of nickel(II) ions onto Chlorella vulgaris. *Process Biochemistry, 38*, 89–99.

Aksu, Z., Egretti, G., & Kutsal, T. (1999). A comparative study for the biosorption characteristics of chromium(VI) on Ca-alginate, agarose and immobilized C. vulgaris in a continuous packed bed column. *Journal of Environmental Science Health A, 34*, 295–316.

Bosinco, S., Dambies, L., Guibal, E., Roussy, J., & Le Cloirec, P. (1997). Removal of Chromium (VI) on chitosan gel beads, Kinetic modeling. *Advances in Chitin Science, 2*, 453–461.

Brady, D., & Duncan, J. R. (1994). Bioaccumulation of metal cations by *Saccharomyces cerevisiae*. *Applied Microbiology & Biotechnology, 34*, 149–154.

Chen, J., & Yiacoumi, S. (1997). Biosorption of metal ions from aqueous solution. *Separation Science and Technology, 32*, 51–69.

Chong, K. H., & Volesky, B. (1995). Description of two-metal biosorption equilibria by Langmuir-type models. *Biotechnology & Bioengineering, 47*, 1–10.

Chui, V. W. D., Mok, K. W., Ng, C. Y., Luong, B. P., & Ma, K. K. (1996). Removal and recovery of copper (II), chromium (III), and nickel (II) from solutions using crude shrimp chitin packed in small columns. *Environmental International, 22*(4), 463–468.

Da Costa, A. C. A., & Leite, S. G. F. (1991). Metals biosorption by sodium alginate immobilized chlorella homosphaera cells. *Biotechnology Letters, 13*, 559–562.

Ding, W., Qing, Lian, Samuels, R. J., & Polka, M. B. (2003). Synthesis and characterization of a novel derivative of chitosan. *Polymer, 44*(2003), 547–556.

Donmez, G., & Aksu, Z. (2002). Removal of chromium(VI) from saline wastewaters by Dunaliella species. *Process Biochemistry, 38*, 751–762.

Grant, G. T., Morris, E. R., Rees, D. A., Smith, P. J. C., & Thom, D. (1973). Biological interactions between polysaccharides and divalent cation: The egg-box model. *FEBS Letters, 32*, 195–198.

Gupta, K. V., Gupta, M., & Sharma, S. (2001). Process development for the removal of Lead and Chromium from aqueous solutions using red-mud-an Aluminum industry waste. *Water Research, 35*, 1125–1134.

Hall, K. R., Eagleton, L. C., Acrivos, A., & Vermeulen, T. (1966). Pore and solid-diffusion kinetics in fixed-bed adsorption under constant-pattern conditions. *Industrial Engineering Chemical Fundamental, 5*, 212–223.

Ho, Y. S. (2003). Removal of copper ions from aqueous solution by tree fern. *Water Research, 37*, 2323–2330.

Ho, Y. S., & McKay, G. H. (2000). The kinetics of sorption of divalent metal ions onto sphagnum moss peat. *Water Research, 34*, 735–742.

Ho, Y. S., Ng, J. C. Y., & Me Kay, G. (2001). Removal of lead (II) from effluents by sorption using second order kinetics. *Separation Science and Technology, 36*, 241–261.

Holan, Z. R., Volesky, B., & Prasetyo, L. (1993). Biosorption of cadmium by biomass of marine algae. *Biotechnology & Bioengineering, 41*, 819–825.

Hsalah, O. J., Weber, M. E., & Vera, J. H. (2000). Removal of Pb, Cd and Zn from aqueous solutions by precipitation with sodium di-(*n*-octyl) Phophinate. *Canadian Journal of Chemical Engineering, 78*, 948–954.

Huang, C., Haung, C. P., & Morehart, A. L. (1990). The removal of Cu(II) from dilute aqueous solutions by *Saccharomyces cerevisiae*. *Water Research, 24*, 433–439.

Ibãnez, J. P., & Umetsu, Y. (2002). Potential of protonated alginate beads for heavy metals uptake. *Hydrometallurgy, 14*, 89–99.

Inoue, K., Baba, Y., Yoshizuka, K., Noguchi, H., & Yoshizaki, M. (1988). Selectivity series in the adsorption of metal ions on a resin prepared by crosslinking copper(II) complexed chitosan. *Chemical Letters*, 1281–1284.

Jang, L. K., Lopez, S. L., Eastmen, S. L., & Pryfogle, P. (1991). Recovery of copper and cobalt by bio polymer gels. *Biotechnology & Bioengineering, 37*, 266–273.

Jiang, N., Chang, X., Zheng, H., He, Q., & Hu, Z. (2006). Selective solid-phase extraction of nickel(II) using a surface-imprinted silica gel sorbent. *Analytica Chimica Acta, 577*, 225–231.

Konishi, Y., Asai, S., Midoh, Y., & Oku, M. (1993). Recovery of zinc, cadmium and lanthanum by biopolymer gel particles of alginic acid. *Separation Science and Technology, 28*, 1691–1702.

Kuyucak, N., & Volesky, B. (1989). Accumulation of cobalt by marine algae. *Biotechnology & Bioengineering, 33*, 809–814.

Lerivrey, J., Dubois, B., Decock, P., Micera, J., & Kozlowski, H. (1986). Formation of D-glucosamine complexes with Cu(II), Ni(II) and Co(II) ions. *Inorganic Chimica Acta, 125*, 187–190.

Leusch, L., Holan, Z. R., & Volesky, B. (1995). Biosorption of heavy metals (Cd, Cu, Ni, Pb, Zn) by chemically reinforced biomass of marine algae. *Journal of Chemical Technology and Biotechnology, 62*(3), 279–288.

Lima, I. S., & Airoldi, C. (2004). A thermodynamic investigation on chitosan–divalent cation interactions. *Thermochimica Acta, 421*, 133–139.

Low, K. S., Lee, C. K., & Tan, K. K. (1995). Biosorption of basic dyes like water, ice huyecinth roots. *Bioresource Technology, 52*, 79–83.

Mimura, H., Ohta, H., Akiba, K., & Onodera, Y. (2001). Uptake behavior of americium on alginic acid and alginate polymer gels. *Journal of Radioanalytical Nuclear Chemistry, 247*, 33–38.

Muzzarelli, R. A. A. (1983). Chitin and its derivatives: New trends of applied research. *Carbohydrate Polymers, 3*, 53–75.

Rangsayatorn, E. S., Upatham, M., Kruatrachue, P., Pokethitiyook, G. R., & Lanza, G. (2002). Phytoremediation potential of Spirulina (Arthrospira) platensis: Biosorption and toxicity studies of cadmium. *Environmental Pollution, 119*, 45–53.

Romero-Gonzalez, M. E., Williams, C. J., & Gardiner, P. H. E. (2001). Study of the mechanism of cadmium biosorption by dealginated seaweed waste. *Environmental Science & Technology, 35*, 3025–3030.

Veera, Boddu M., Krishnaiah, A., Jonathan, Talbot L., & Edgar, Smith D. (2003). Removal of hexavalent chromium from wastewater using new composite chitosan biosorbent. *Environmental Science & Technology, 37*, 4449–4456.

Volesky, B. (2003). Biosorption process simulation tools. *Hydrometallurgy, 71*, 179–190.

Volesky, B. (1999). Biosorption for the next century. In *Proceedings of the International Biohydrometallurgy Symposium*. Spain: El. Escorial.

Wu, F. C., Tseng, R. L., & Juang, R. S. (2000). Comparative adsorption of metal and dye on flake- and bead-types of chitosans prepared from fishery wastes. *Journal of Hazardous Materials, 73*, 63–75.

Yang, Z., & Yuan, Y. (2001). Studies on the synthesis and properties of hydroxyl azacrown ether-grafted chitosan. *Journal of Applied Polymer Science, 82*, 1838–1843.

Zhang, L. M., & Chen, D. Q. (2002). An investigation of adsorption of lead(II) and copper(II) ions by water-insoluble starch graft copolymers. *Colloids & Surface A, 205*, 231–236.

Zouboulis, A. I., Matris, K. A., Lanara, B. G., & Nescovic, C. L. (1997). Removal of Cd from dilute solutions by hydroxyl apatite (II) Floatation studies. *Separation Science and Technology, 32*, 1755–1767.